Experimental study and phenomenological modelling of flaw sensitivity of two polymers used as dielectric elastomers

Dilshad Ahmad[a], Karali Patra[a,*], Mokarram Hossain[b]

[a]*Department of Mechanical Engineering, Indian Institute of Technology Patna, Patna-800013, India*
[b]*Zienkiewicz Centre for Computational Engineering, College of Engineering, Bay Campus, Swansea University, Swansea, UK*

Abstract

The extreme stretching of dielectric elastomers in sensors, actuators, and energy harvesting devices is a common phenomenon where the materials are prone to fracture under the influence of flaws and notches. In this work, we have investigated the length of flaw sensitivities of two widely used dielectric materials, acrylic (VHB) and silicone (Ecoflex) elastomers under a pure shear loading and established that the length of flaw sensitivity of acrylic is almost double than that of silicone. Therefore, the acrylic elastomer is safer to operate for small notches as compared to the silicone material. However, within the flaw sensitive length, failure stretch, fracture toughness and failure stress are more for Ecoflex than those for VHB. It is found that the failure stretch and the fracture toughness decrease drastically after the length of flaw sensitivities for both materials. Also, the failure stress keeps on decreasing with an increasing notch length for both materials. Afterwards, a simple phenomenological relation is proposed for fitting experimental results under a pure shear loading with only two parameters. The mathematical relation is valid for both the materials and covers the notch sensitivity with a good agreement.

Keywords: Dielectric elastomer, stretchability, length of flaw sensitivity, pure shear, fracture toughness.

1. Introduction

Highly stretchable dielectric elastomers (DEs) are increasingly becoming popular due to their wide applications in the field of sensors, actuators, and energy harvesting devices [1, 2, 3, 4, 5, 6, 7, 8, 9, 10, 22]. Similar to other elastomers, DE generally deforms in three fundamental ways: simple extension [11, 12], equibiaxial extension [13, 14] and pure shear (laterally constrained) [15, 16, 17, 18]. Simple extension is the most fundamental method of deformation in which the length to width ratio of the material is kept high [19, 20, 21, 23, 24]. For a homogeneous uniaxial deformation, the material elongates along its length direction maintaining the width free to contract [11]. Equi-biaxial is another popular method of deformation in which the material is stretched from both (length and width) mutually perpendicular sides [25, 26]. This mode of deformation involves numerous application areas because of its compatibility and higher efficiency. Recently, the pure shear deformation mode has gained importance in which the width direction is not allowed to contract while the material is stretched in the length direction. Therefore, due to its compatibility, efficiency and easier pre-stretching ability, this mode of deformation attracted scientists and researchers to

*Corresponding author. +91-612-255-2012
Email addresses: dilshad.pme14@iitp.ac.in (Dilshad Ahmad), kpatra@iitp.ac.in (Karali Patra), mokarram.hossain@swansea.ac.uk (Mokarram Hossain)

develop efficient and compatible actuators and energy harvesting devices [17, 27].

Note that the efficiency and functioning of sensors, actuators and energy harvesting devices are largely depending upon the ability of dielectric elastomer to stretch before any failure commonly known as stretchability. But notches and flaws present in DE materials affect the performances of devices and reduce the stretchability markedly [15]. Notches may vary from flaws (very small) to larger cuts. Flaws may be present in the pristine material during synthesis but larger cuts may be introduced during fabrication or during the applications as different devices. In the earlier works both pristine and larger notched specimen were tested under various conditions [15, 16]. Pristine samples under a uniaxial loading were tested for different elastomers and their failure envelopes were compared by Smith [27]. It was found that silicone had a smaller failure stretch and natural rubber had somewhat a larger failure stretch than the vulcanizates of the three other rubbery polymers [28]. A complete fracture of smooth specimens under multiaxial quasi-static loadings using unfilled and carbon black filled elastomers was investigated by Hamdi et al. [14] and a criterion based upon an equivalent elongation was proposed and experimentally validated for various loading paths. Fan et al. [29] investigated the fatigue failure of DEs under a cyclic loading by fixing their maximum stretch up to 4.5 under a pure shear loading. Schmidt et al. [12] investigated the stretchability of the pristine dielectric elastomer that was limited around 9.0 for all three kinds of deformation modes, uniaxial, pure shear, and equi-biaxial.

It has been observed that the stretchability or the failure stretch of DE materials goes very high up to 1000% under a pure shear stretching but it drops markedly down to 400% with the introduction of larger notches [15]. In our earlier work [30], we also investigated the stretchabilty of commercially available and widely used VHB 4910 for different notch lengths which were more than 20% of the width of the pure shear samples. It was observed that the stretch at failure did not vary much with the increasing notch lengths in the pure shear condition. Kaltseis et al. [16] also conducted pure shear tests on three different materials and found that the stretchability for VHB reduced down to 3.5 from 9.5 in a pristine sample when a larger notch (20% of width) was introduced. Similarly, the stretchabilty reduced from 6.0 to 1.75 for Oppo band (natural rubber) and from 5.0 to 1.25 for ZRU (natural rubber). Wang et al. [31] predicted the stretchability of swollen dielectric elastomers under a simple extension and found that the stretch at failure decreased considerably with the increasing notch length from smaller to larger.

Some of the researchers investigated the length of flaw sensitivity over which the material becomes notch sensitive, i.e., a sudden drop of stretchability of the material. When the stretchability of elastomers is reduced significantly under the influence of notches and flaws, the phenomenon is termed as the flaw sensitivity. Setua et al. [32] conducted experiments under a uniaxial loading to see the effects of silk fibre, ageing, reinforcing carbon black filler and elevated temperature on the length of flaw sensitivity of rubber vulcanizates. It was found that the length of the flaw sensitivity increased with the increasing short fibres. On ageing, the critical length values for composites increased while those for unfilled vulcanizates decreased. The length of flaw sensitivity for the fibre reinforced composites at a higher temperature remained unchanged, but dropped in the case of unfilled vulcanizates. Akhtar et al. [33] investigated the short silk fibre filled thermoplastic elastomer blends from low-density poly-ethylene and natural rubber (NR) containing pre-cuts of different lengths and found that unlike vulcanized NR, no length of flaw sensitivity was found in the case of both blends and unvulcanised NR. Hamed [34] successfully investigated the effect of cross-link density on the critical flaw size of a simple elastomer gum amorphous EPDM (Epsyn 70 A) under a uniaxial loading. It was precisely concluded that the length of flaw sensitivity decreased with the increasing cross-link density.

After a comprehensive literature review presented above, it is clear that many researchers conducted tests on rubbers under the uniaxial loading with varying notch lengths from very small to very large but only few has investigated the length of the flaw sensitivity for DEs applied as stretchable transducers. Very recently, Chen et al. [35] investigated the notch sensitivity of dielectric elastomer (VHB polymer) under a uniaxial load and proposed a method to calculate the length of flaw sensitivity of highly stretchable polymers. They maintained the length to width ratio to at least 2 while varying the length of notch. Also, the length of notch is maintained at 5 times smaller than the width of the sample.

Understanding the length of flaw sensitivity is of significant importance because operating DEs within the flaw length will not affect the stretchability of the transducer materials. To the best of the authors' knowledge, except on the highly viscous VHB polymer used for DEs, there is no study to determine the length of flaw sensitivity on other less viscous DEs, e.g., Ecoflex/silicone polymers. In the work of Chen et al. [35], it can be seen that they have taken specimens with different notch lengths. However, this study is conducted under a uniaxial type of deformation. Further study is required under a pure shear deformation for several reasons. Firstly, since the pure shear mode of deformation is widely used in DE-made devices due to its better electromechanical performances and easy for implementation, it is worth to investigate the length of flaw sensitivity of DEs under a pure shear configuration. Secondly, Chen et al. [35] used samples where the notch c ranging from $\sim$ 0.05 to 50 mm and the width w is at least 5 times the notch length. Therein, the length is at least twice the width, varying case by case. The effects of different notch lengths on stretchability and fracture toughness under a uniaxial loading are rather vague as with increasing the width its length is also increased. Therefore, it is better to adopt a different form of deformation where the width is large enough to introduce notches in a single specimen maintaining the same width and height. For that the pure shear is the ideal loading condition where the width is almost 14 times more than length and it is not varying case by case. Therefore, to calculate the stretchability, fracture energy and stretchability with a larger cut, a pure shear method is adopted by Pharr et al.[15]. We have also chosen this method for the same reason. The stress-stretch curve patterns for uniaxial, pure shear and equibiaxial are different [12] under the same condition. Therefore only doing uniaxial test and making it valid for other loading condition is not a good idea [36] especially for the notch sensitive investigation where in the pure shear loading the width is unable to contract more than 2% while stretching. In uniaxial loading, the width continuously contracts while stretching. On the one hand, the stress acting at a particular stretch will always be more in the pure shear as compared to uniaxial case [36]. On the other hand, the strain energy density (area under the stress-stretch curve) of elastomers should be equal irrespective of modes of deformation. Therefore, pure shear deformation will have less stretchability and fails early as compared to a uniaxial to keep the strain energy density equal. Moreover, pure shear mode of deformation has the advantage of creating larger active areas providing more compatibility for sensors, actuators, and energy harvesting applications [37, 38, 39].

Moreover, due to highly dissipative behaviours of VHB polymer, other soft polymers have also been widely used in DE devices. For example two parts Ecoflex silicone from Smooth-On Company (USA) has been used in soft robotics. Therefore, in the present work, the length of flaw sensitivity is investigated for the first time for two elastomeric materials namely, VHB 4910 and Ecoflex under a pure shear mode by constraining sample configurations laterally. It has been experimentally established that the length of flaw sensitivity of the VHB 4910 is almost double than that of Ecoflex and hence the former is safer to operate. It is successfully investigated that both failure stretch and fracture toughness decrease drastically after the notch length exceeds the length of flaw sensitivities for both materials. The failure stress also keeps on decreasing with

the increasing notch length. To the best of our knowledge, this is the first experimental investigation for the length of flaw sensitivities under a pure shear loading on highly stretchable materials. Furthermore, in order to capture the experimental findings, we develop a simple mathematical relation that fits the relevant experimental data with a quite good agreement.

This paper is organized as follows: Section 2 explains the experimental details including material syntheses, sample preparations and experimental procedures. In Section 3, a detailed discussion is presented explaining the experimental outcomes while a simple but accurate phenomenological model correlating the failure stretch and the flaw length is presented in Section 4. A final Section 5 presents a brief summary of the current work.

2. Experimental details

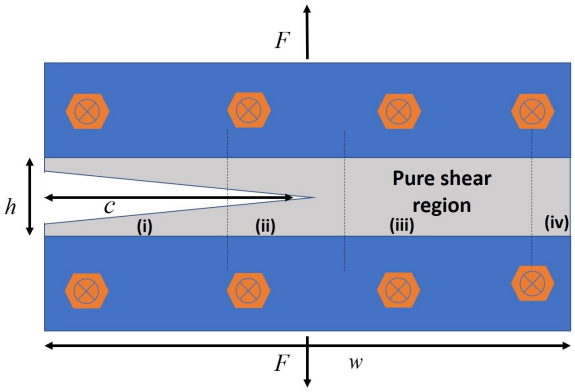

Figure 1: Specimen with a notch showing pure shear region

2.1. Materials

Two dielectric materials are used in the current experimental study. One is commercially available acrylic elastomer (VHB 4910) purchased from 3M company. The thickness of the material is 1 mm. Second one is Ecoflex silicone polymer which is prepared in our laboratory. For the preparation of Ecoflex, Part A and B of the material (manufactured by Smooth-On, USA) are mixed in equal proportion to get the sheet of required thickness. The Ecoflex sheet is allowed to cool in an open environment at room temperature for 24 hours in order to make the thickness of the sheet uniform. The thickness of the sheet is then measured at different positions by using a digital thickness gauge to confirm uniform thickness of 0.63 mm $\pm 0.05 \mu$m. The designed and fabricated mould is shown in Figure 2.

2.2. Experimental procedures

Both the materials (VHB 4910 and Ecoflex) are tested in a pure shear deformation mode on an Universal Testing Machine (UTM) of Zwick/Roell where the ultimate load capacity of the load cell is 2.5 kN. To ensure a proper pure shear mode, a customised fixture compatible with the 2.5 kN load cell is used, cf. Figure 3. To keep the specimen laterally constrained, the width and the height of VHB material are taken

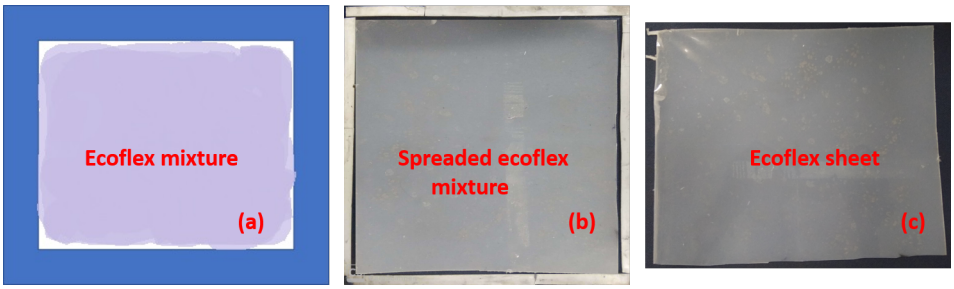

Figure 2: (a) Designed mould with ecoflex mixture (b) fabricated mould with spreaded Ecoflex mixture (c) prepared Ecoflex sheet

to be 320 mm and 17 mm, respectively while for the Ecoflex material, these are to be 140 mm and 10 mm, respectively. In this way, the width to height ratios for both the materials are well above 10 to ensure a pure shear deformation [15].

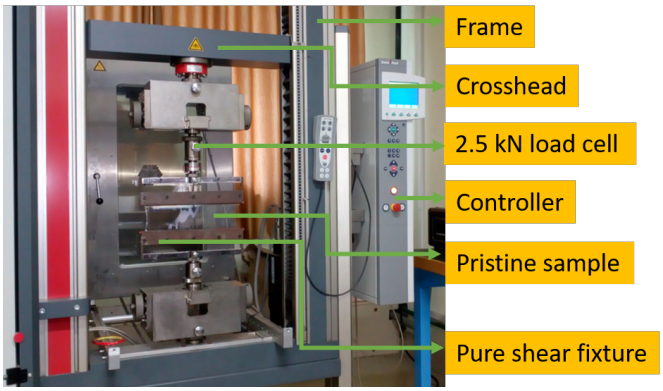

Figure 3: Experimental set up showing a pristine specimen on a pure shear fixture

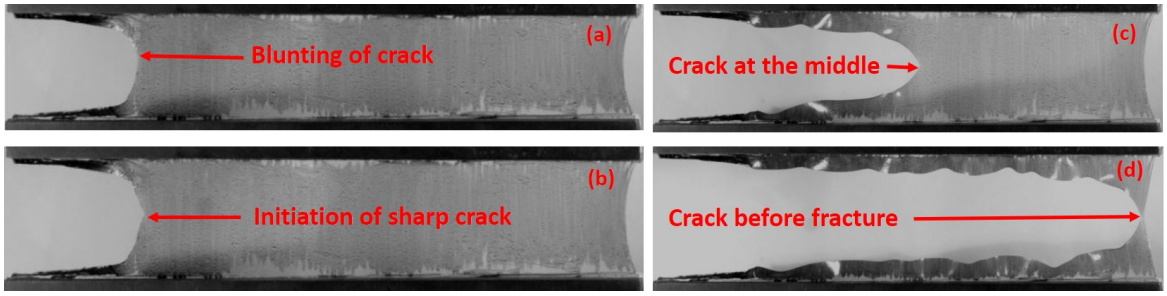

Figure 4: (a) Blunting of 64 mm length crack of VHB under a pure shear loading at a strain rate of 10/min (b) initiation of crack tip (c) propagation of crack at the middle of a specimen (d) crack just before fracture

To prevent slippage of the sample we used sand paper inside the fixture and then tightened it with bolts. Notches with different lengths have been created systematically into the sample using a surgical scissor. A

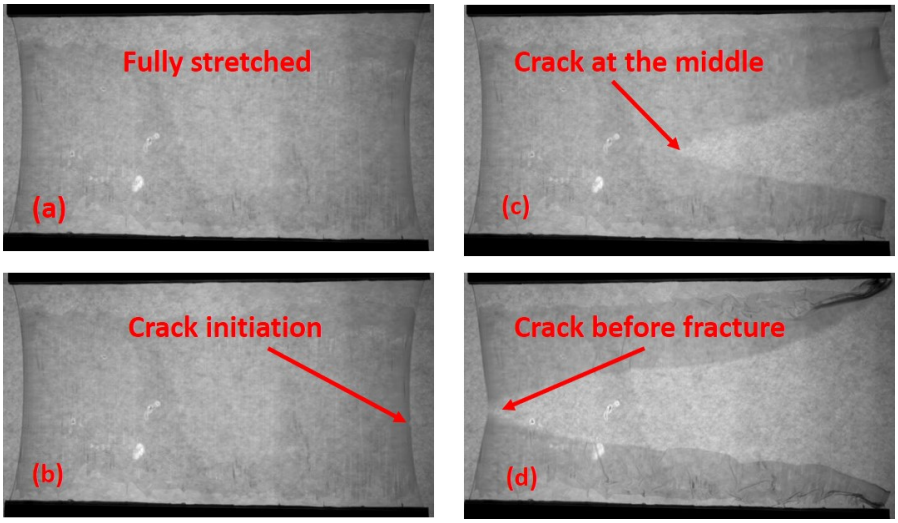

Figure 5: Fully stretched VHB pristine sample at 10/min strain rate (b) crack initiates from the arbitrary flaw (c) crack reaches at the middle of the specimen (d) crack just before the fracture of the specimen

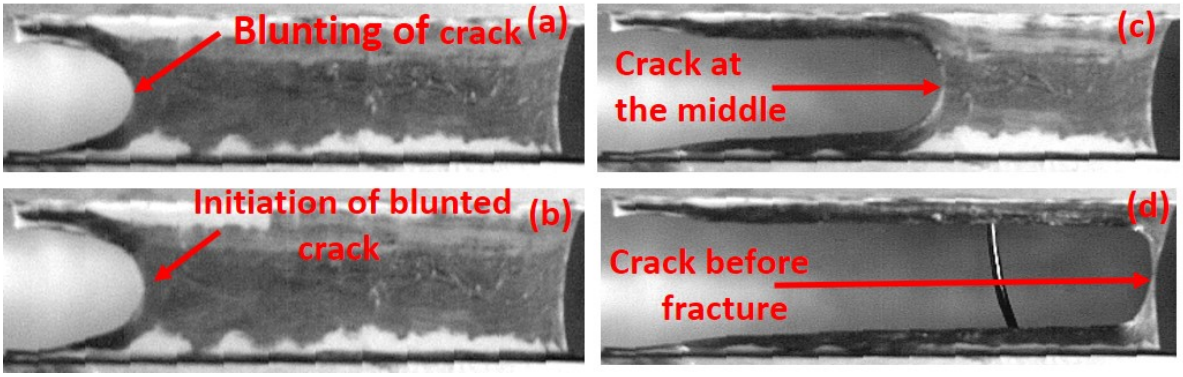

Figure 6: (a) Blunting of 30 mm long notch of Ecoflex specimen under a pure shear loading at a strain rate of 10/min (b) initiation of blunted crack (c) propagation of crack at the middle of a specimen (d) crack just before fracture

pure shear specimen with a larger notch is shown in Figure 1. A notch is created in the specimen which is half the length of the width. There are generally four regions in the pure shear specimen [40] which are marked as (i), (ii), (iii) and (iv) in Figure 1. In region (i), the strain energy in the specimen is negligible while the region (ii) is a complicated state of strain where the strain energy is difficult to determine. The region (iii) is a pure shear region in which the specimen is fully in laterally constrained state and hence termed as the pure shear region. Furthermore, in region (iv), the strain energy is negligible as it is a force free region. In the present work, we have kept the width to height ratio of both the materials as high as 14 so that even after creating a larger notch (half the width), the rest half of the specimen remains laterally constrained. Hence, it is ensured that a specimen remains under a pure shear deformation even after the introduction of the largest cut (half of width) as clearly shown in Figure 1.

Pristine and notched samples are then stretched by a uniaxial force at a strain rate of 10/min. Images are

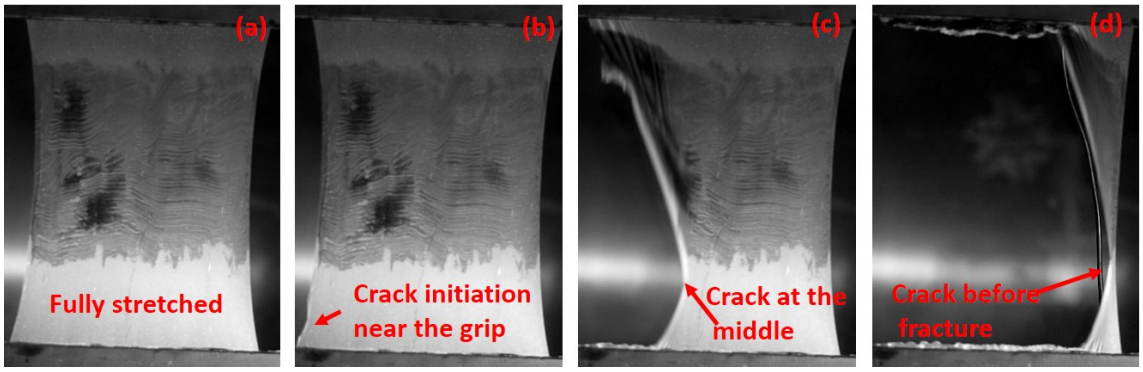

Figure 7: (a) Fully stretched Ecoflex pristine sample at 10/min strain rate (b) crack initiates from the maximum stress concentration near the grip (c) crack reaches at the middle of the specimen (d) crack just before the fracture of the specimen

taken with the help of a high-speed camera (Vision Research, USA). The crack propagation of notched samples for VHB 4910 are shown in Figure 4. A 64 mm notch length is created in the sample with a scissor and then it is allowed to be stretched at a strain rate of 10/min. Then blunting of notch takes place as the specimen elongates as shown in Figure 4(a) after which a sharp crack tip initiates as shown in Figure 4(b) and starts to propagate. Figure 4(c) shows the propagation of a crack up to the middle of the specimen. A crack that is initiated just before the fracture is shown in Figure 4(d) and finally the sample tears into two parts.

Now, a pristine sample of VHB under a fully stretched condition is shown in Figure 5(a) in the absence of any specified notch. The fully stretched condition is the maximum stretch of a sample before any rupture. In this case, a sharp crack develops from any flaw which may present in arbitrary position as shown in Figure 5(b) [35]. Figure 5(c) illustrates the propagation of a crack when it almost reaches at the middle of the sample. In Figure 5(d), it has been observed that the crack reaches at the end just before any fracture. Finally, the complete fracture of the material takes place in a fraction of second.

In a similar way notched samples for Ecoflex are also stretched at 10/min. In Figure 6(a) blunting of 30 mm crack created in 140 mm specimen of Ecoflex is shown. Here the crack developed is blunted in shape as shown in 6(b) and this blunted crack then propagates and reaches the middle of the sample as shown in 6(c). Finally the crack reaches at the other end before fracture, see 6(d). Also the fracture of pristine Ecoflex sample is illustrated in Figure 7. Here, a fully stretched Ecoflex specimen just before formation of any crack is shown in Figure 7(a). The formation of blunted crack in this case happens near the grip where the maximum stress concentration is encountered [26] as clearly shown in 7(b). This blunted crack is shown at the middle of the sample illustrated in Figure 7(c) which finally reaches at the end of the sample just before complete fracture of the specimen, see 7(d).
So far, a systematic investigation of the notch sensitivity under a pure shear loading for both materials has been demonstrated. We have calculated the length of flaw sensitivity using pristine and larger notched specimens. The length of flaw sensitivity L_f can be defined as in Chen et al. [35]:

$$L_f = \frac{J_c}{W^*} \tag{1}$$

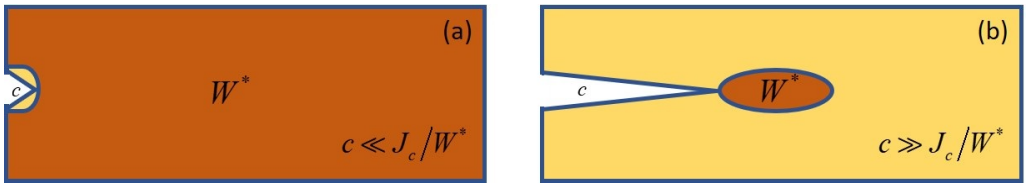

Figure 8: Strain energy density for (a) a pristine sample or a small notched specimen (b) a larger notched specimen at a fixed strain rate.

where, J_c is the fracture toughness for a larger notched length specimen (kJ/m^2) and W^* is the strain energy density of the pristine specimen or very small notched specimen (MJ/m^3). The fracture toughness J_c is calculated using the following equation generally used for the elastomeric materials [41]:

$$J_c = \frac{U_c}{b[w-c]} \tag{2}$$

where, U_c = area under a force-displacement curve of the notched specimen, b = thickness of the specimen, w = width of the specimen, c = notch length in the specimen. The advantage of using Equation (2) to calculate the fracture toughness is that it requires only one sample to be tested which makes the calculation much easier [41] because generally, for pure shear loading two specimens are used to measure the fracture energy of the elastomers [15]. First the notched specimen is tested to see the failure stretch and then pristine specimen is loaded up to same failure stretch to get the stress-stretch curve. In the present case for equation 2, one sample is advantageous because it reduces time consumption and cost appreciably. As shown in Figure 8, if the notch length c is less than the length of the flaw sensitivity L_f, then the work done to rupture the material is stored in the whole specimen which is quite high. If the notch length c is comparatively larger, then the work done to rupture the material is confined around the tip of the crack which is remarkably less. The fracture toughness J_c is calculated for VHB and Ecoflex materials with a larger notched specimen using Equation (2). Numerical values of the fracture toughness J_c for VHB and Ecoflex are found to be 3.5 kJ/m^2 and $1kJ/m^2$, respectively; while, the values of strain energy densities W^* for these materials are $1.66MJ/m^3$ and $2.14MJ/m^3$, respectively. Note that W^* is calculated by dividing U_c^* with the volume of the sample ($w \times b \times h$) as shown in Figure 8 and by using Equation (3). Force-displacement curves are shown in Figure 9(a) and 9(b) for VHB and Ecoflex, respectively. In Figure 9(a), force-displacement curves are shown for both pristine and larger notched (20% of width) VHB 4910 specimens under a pure shear loading. In Figure 9(b), force-displacement curves for both pristine and larger notched Ecoflex specimens are shown. For the present experimental set up, L_f is coming around 2 mm and 0.43 mm for VHB and Ecoflex, respectively, which are well reasonable in the range for elastomeric materials [35],

$$W^* = \frac{U_c^*}{[w \times b \times h]}, \tag{3}$$

where, W^* = strain energy density of a pristine specimen, U_c^* = area under the force-displacement curve of a pristine specimen.

3. Results and discussions

3.1. Experimental analysis

The stress-stretch curves for different notch lengths and pristine samples for two different materials at a strain rate of 10/min are depicted in Figure 10. Five experiments are conducted for each case and one best is chosen to represent the stress-stretch behaviour of a material. Total eleven notches are created out of which only eight different notched specimens are shown in order to see the pattern clearly. The width of the VHB specimen is taken to be 320 mm, thickness is 1 mm the height is 17 mm to ensure the width to height ratio of 18. Similarly, the width of the Ecoflex material is 140 mm, thickness is 0.63 mm the height is taken as 10 mm that ensures the width-height ratio to be 14. The stress is calculated by dividing force with initial area of the specimen. Initial areas of VHB and Ecoflex specimens are 320 mm^2 and 88.2 mm^2, respectively.

For pristine (c≈0.0001 mm) and smaller notched samples (1 mm, 2 mm) in VHB 4910 as shown in Figure 10(a), it is observed that the stress-stretch curves are almost similar. For medium notches (5 mm and 8 mm), the stress-stretch curves are showing a decrease in failure stretch values and for larger notched samples (64 mm-160 mm) when the failure stretch becomes minimum, there is no change in the failure stretch value. A similar pattern is obtained for the Ecoflex material as shown in Figure 10(b). For pristine ($c \approx 0.0001$ mm) and smaller notched specimens (0.2 mm and 0.4 mm), the stress-stretch behaviour is similar and the failure stretches are almost constant. But for medium notches (1 mm and 5 mm), the failure stretches decrease and for larger notches (30 mm-70 mm), the failure stretches remain constant. In general, naturally occurring flaws are present in $30 \pm 20\mu m$ range in elastomers [32, 33]. Therefore, in the current work, a flaw of 0.001 mm is considered as the lowest flaw length for both VHB and Ecoflex so that the phenomenological model is valid for any possible size of flaw. This flaw length is then normalized by dividing with the initial width of the specimen in both cases. The normalized notch lengths have therefore come in the range of 10E-7. We have plan to compare our experimental data under this study with numerical simulations in a forthcoming contribution. In Figure 11(a), the failure stretch versus the normalised notch length is plotted for VHB and Ecoflex materials. All the tests are conducted minimum five times to ensure a good reproducibility. The vertical error bars show standard deviations of these measurements. The normalised length of flaw sensitivity L_f is found to be 2 mm (0.00656) and 0.4 mm (0.00285) for VHB and Ecoflex, respectively, at a strain rate of 10/min. For VHB, the average stretch at rupture almost remains constant at about 9.0 when the notch in the specimen is less than 2 mm (0.00656). For Ecoflex, the average stretch at failure is about 12.5 when the notch in the specimen is less than 0.4 mm (0.00285). The notch sensitive region lies between c = 2 mm (0.00656) to c = 32 mm (0.1) for VHB and the same lies between c = 0.4 mm (0.00285) to c = 10 mm (0.071) for Ecoflex as shown in Figures 11(a) and 11(b), respectively. Note that c=32 mm and c=10 mm are the maximum values of the flaw sensitivity for VHB and Ecoflex, respectively. We have seen that the normalized length of flaw sensitivity for VHB (0.00656) is almost double than that of Ecoflex (0.00285). Here, notch lengths are normalized to compare between the two materials as widths of VHB and Ecoflex are different, i.e., 320 mm and 140 mm, respectively. This investigation has established that Ecoflex is more prone (almost double) to fracture at a smaller notch length than that of VHB under a pure shear loading.

It is clearly seen that when the notch length is less than L_f, the stretch at failure is insensitive to notch lengths but when the notch length is more than L_f, the stretch at failure is sensitive to notches and finally reaches up to a lowest value at a larger cut limit. Physically, this is because the stretch at rupture depends on the fracture toughness stored in the sample whose variation with the normalized notch length is shown in Figure 11(b). It can clearly be observed from Figure 11(b) that for VHB, the average fracture toughness of pristine samples

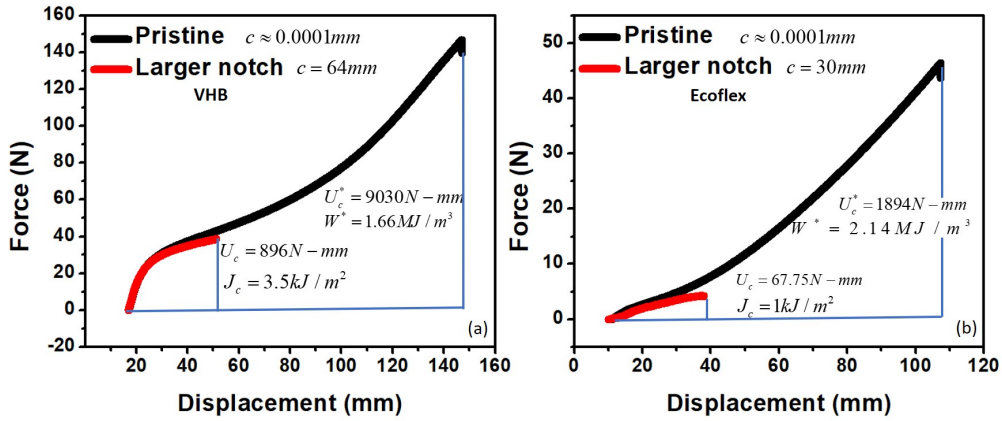

Figure 9: Force versus displacement graphs for pristine and larger notched specimens for (a) VHB (b) Ecoflex

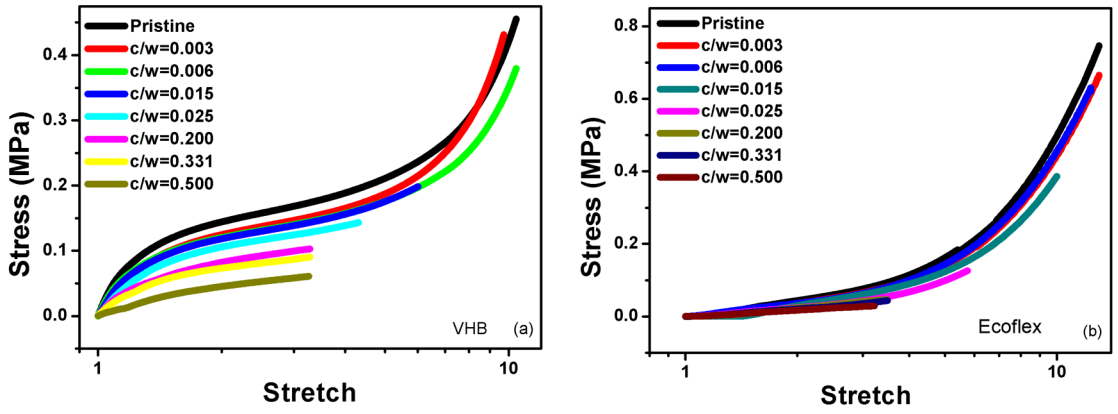

Figure 10: Stress-stretch curves for different notch lengths for (a) VHB and (b) Ecoflex materials under a pure shear loading

is around 20 kJ/m^2 and it remains unchanged with the change in the normalized notch length up to a particular value. But after the normalized notch length of 0.00656, it is seen that the fracture toughness decreases with an increase of the normalized notch length till it reaches 0.0625 and then remains constant at around 3.5 kJ/m^2. In a similar way, the fracture toughness of the pristine specimen of Ecoflex material varies with the normalized notch length. The fracture toughness of the material is 22 kJ/m^2 which remains constant till the normalized notch length of 0.00285. After this value, the fracture toughness shows a declining curve up to the normalized notch length of 0.0625 and then becomes constant to $1kJ/m^2$ for a higher normalized notch length. This is because the strain energy density is stored in the whole specimen for a pristine sample which induces a higher fracture toughness in the specimen. However, for larger notch lengths, the strain energy density is stored only at the tip of the crack which enables lesser fracture toughness as shown in Fig-

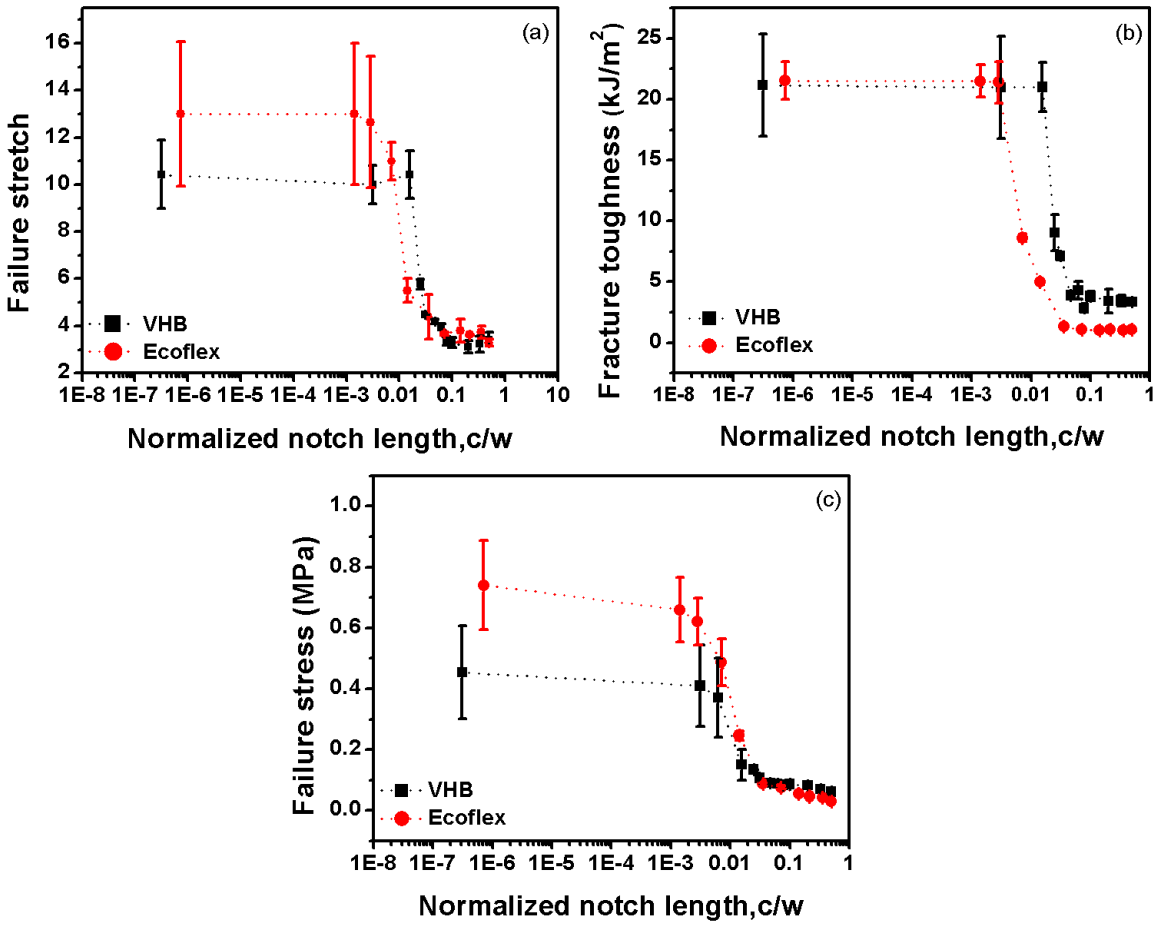

Figure 11: (a) Stretch at failure (b) fracture toughness and (c) failure stress with normalized notch lengths

ure 9. The fracture toughness of the Ecoflex material is considerably less as compared to the VHB at larger notches. This can be explained from Figure 9, where it is clearly shown that the area under the stress-stretch curve obtained for VHB is always more than that for Ecoflex. The area under the force-displacement curve of a pristine specimen, U_c^* for VHB and Ecoflex are 9030 N-mm and 1894 N-mm, respectively for the same strain rate while U_c are 896 N-mm and 67.75 N-mm, respectively. The same pattern is observed while comparing Figures 10(a) and 10(b) where the stress-stretch curve is always greater for VHB than for Ecoflex. The failure stress with the normalized notch length shows a decreasing trend as shown in Figure 11(c). For VHB, the failure stress of the pristine sample is high up to 0.42 MPa that keeps on decreasing to 0.05 MPa for a normalized notch length of 0.5. In contrast, the failure stress of Ecoflex material is 0.78 MPa which is comparatively higher than that of VHB and decreases up to 0.04 MPa for a normalized notch length of 0.5.

The maximum stress at which a material fails is termed as the failure stress. The failure stress is decreasing

with increasing notch length because the stress-stretch curve areas as depicted in Figure 10 are showing a constant decrease with increasing the notch length. The strain energy density stored in the specimen decreases with increasing notch length causing decrease in the failure stress. Within L_f, the failure stress for Ecoflex is higher than that of VHB. This is because the strain energy density is always higher for Ecoflex than that of VHB for smaller notches as shown in Figure 10. However, L_f of Ecoflex is lesser than VHB, therefore the failure stress sharply starts decreasing earlier for Ecoflex than VHB resulting the failure stress for Ecoflex to be lower than VHB at larger normalized notch lengths as shown in Figure $11(c)$. Hence for larger normalized notch lengths, the failure stress for Ecoflex becomes lower than that of VHB because the strain energy density at larger normalized notches are comparatively lesser for Ecoflex than that of VHB.

4. A phenomenological model for failure stretch and notch length

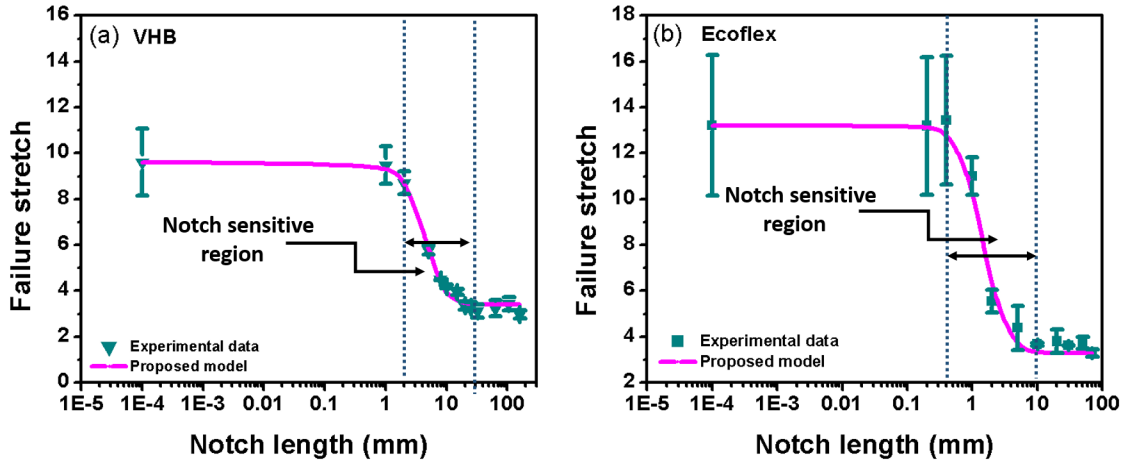

Figure 12: Experimental data fitted with the proposed model for (a) VHB (b) Ecoflex

In the previous section, it is discussed that the failure stretch remains constant for a certain length of notch termed as the length of flaw sensitivity. After that the specimen becomes notch sensitive till it reaches up to a larger notch. At larger notches, the failure stretch again becomes constant under a pure shear loading. This transition occurs when the notch length c becomes equal to the critical value $L_f = J_c/W^*$. When c becomes smaller than L_f, the failure stretch is insensitive to the notch length but when the notch length is more than L_f, the failure stretch decreases and finally becomes a constant at larger notches. In order to capture this transition, we propose a relation between the fracture stretch and the notch length as,

$$\lambda_f = \frac{[\lambda_{\text{max}} - \lambda_{\text{min}}]}{1 + \left[\frac{cW^*}{xJ_c}\right]^n} + \lambda_{\text{min}}, \tag{4}$$

where, λ_{max} = maximum stretch of the pure shear specimen, λ_{min} = minimum stretch at larger notches, W^*

= strain energy density at larger notches, J_c = fracture toughness at large notches, c = length of a notch, x = correction factor depends upon the length of flaw sensitivity, n = variable depends upon the stiffness of the material. Less stiff material is having high value of n and high stiff material is having low value of n. There are two limits set in the above equation. For small notch/flaws limit, as $c \to 0$, $\lambda_f \to \lambda_{\text{max}}$ and for a larger notch limit as $c \to \infty$, $\lambda_f \to \lambda_{\text{min}}$. A transition occurs when the notch length c approaches the length of flaw sensitivity L_f, i.e., $c \to L_f$. This phenomenological relation works well for smaller and larger notches where the transition occurs at $c = J_c/W^*$.

The proposed empirical equation fits well with the experimental results for both the materials as shown in Figure 12. In Figure 12(a), the experimental failure stretch values for VHB are shown by dark cyan scattered data with standard deviations. Note that within the flaw length, the size of notches/flaws are very small. Hence it is very difficult to control the exact size of notches in this region. Therefore, the stretchability varies appreciably within the region of flaw length which in turn causes a high standard deviation. After the flaw length, we are able to control the exact size of notches causing a reduced standard deviation. We have proposed a simple phenomenological relation with two unknowns n and x as shown in Equation (4). This equation is showing better fitting with both VHB and Ecoflex materials. The magenta line is showing the proposed phenomenological model which is simple but accurate and shows better fitting with all smaller, intermediate and larger notches under a pure shear deformation. Eleven notches are created in both VHB and Ecoflex specimens. Three notches are shown within the flaw length (L_f). Creating a greater number of notches/flaws within the flaw length will not affect the fitting of the proposed model. Because the stretchability remains constant within the flaw length and the proposed model is fitted very well with all eleven experimental data for both the materials. The values of two constants n and x obtained through the experimental data fitting of VHB material are 3.24 and 18, respectively. From Figure 12(b), it is seen that the experimental failure stretch for Ecoflex material is fitted well with our proposed model. The constants n and x are 3.4 and 3.11, respectively.

5. Conclusion

In the application areas of dielectric elastomers, the pure shear deformation is one of the most commonly used methods of stretching. Therefore, this work analyses the length of flaw sensitivity of two highly stretchable dielectric materials (VHB and Ecoflex) under a pure shear loading. The length of flaw sensitivity for VHB is found to be double of the Ecoflex material and hence the former is safer to operate even with small notches. Within this flaw sensitive length, failure stretch, fracture toughness, and failure stress are more for Ecoflex than for VHB. It is found that failure stretch, fracture toughness, and failure stress decrease drastically after the notch length exceeds the respective length of flaw sensitivities for both materials. Moreover, a simple mathematical relation is proposed for fitting experimental results under a pure shear loading with only two parameters. This phenomenological formula is fitted for both the materials and covers the notch sensitivity with a very good accuracy.

6. Acknowledgement

The work was partially supported by DST, Government of India under a research project No. INT/SIN/P-03

References:

[1] An L, Wang F, Cheng S, Lu T and Wang T J. *Experimental investigation of the electromechanical phase transition in a dielectric elastomer tube*. Smart Mater. Struct. 24 :035006, 2015

[2] Zhang C, Chen H, Liu L and Li D. *Modelling and characterization of inflated dielectric elastomer actuators with tubular configuration*. J. Phys. D. Appl. Phys. 48: 245502, 2015.

[3] Mathew A T and Koh S J A. *Operational limits of a non-homogeneous dielectric elastomer transducer*. Int. J. Smart Nano Mater. 8: 214?231, 2017.

[4] Sahu R K, Saini A, Ahmad D, Patra K and Szpunar J. *Estimation and validation of maxwell stress of planar dielectric elastomer actuators*. J. Mech. Sci. Technol. 30: 429-436, 2016.

[5] Saini A, Ahmad D and Patra K. *Electromechanical performance analysis of inflated dielectric elastomer membrane for micro pump applications*. Process. SPIE 9798: 979813, 2016.

[6] Kumar A, Ahmad D and Patra K. *Dependence of actuation strain of dielectric elastomer on equi-biaxial, pure shear and uniaxial modes of pre-stretching*. IOP Conf. Ser. Mater. Sci. Eng 310: 012104, 2018.

[7] McKay T G, O'Brien B M, Calius E P and Anderson I A. *Soft generators using dielectric elastomers*. Appl. Phys. Lett. 98: 1-4, 2011.

[8] Zhao X and Suo Z. *Theory of dielectric elastomers capable of giant deformation of actuation*. Phys. Rev. Lett. 104: 1-4, 2010.

[9] Koo I M, Jung K, Koo J C, Nam J and Lee Y K. *Development of Soft-Actuator-Based Wearable Tactile Display*. IEEE Trans. Robot. 24: 549-558, 2008.

[10] Slesarenko V, Engelkemier S, Galich P, Vladimirsky D, Klein G, Rudykh S. *Strategies to control performance of 3D-printed, cable-driven soft polymer actuators: From simple architectures to gripper prototype*. Polymers, 10(8): 846, 2018.

[11] Cohen N, Oren S S and deBotton G. *The evolution of the dielectric constant in various polymers subjected to uniaxial stretch*. Extrem. Mech. Lett. 16: 1-5, 2017.

[12] Schmidt A, Rothemund P and Mazza E. *Multiaxial deformation and failure of acrylic elastomer membranes*. Sensors Actuators, A Phys. 174: 133-138, 2012.

[13] Huang J, Shian S, Suo Z and Clarke D R. *Maximizing the energy density of dielectric elastomer generators using equi-biaxial loading*. Adv. Funct. Mater. 23: 5056-5061, 2013.

[14] Hamdi A, Nait A M, Ait H N, Heuillet P and Benseddiq N. *A fracture criterion of rubber-like materials under plane stress conditions*. Polym. Test. 25: 994-1005, 2006.

[15] Pharr M, Sun J Y and Suo Z. *Rupture of a highly stretchable acrylic dielectric elastomer*. J. Appl. Phys. 111, 2012.

[16] Kaltseis R. *Natural rubber for sustainable high-power electrical energy generation*. RSC Adv. 4: 27905-27913, 2014.

[17] Koh S J A. *High-performance electromechanical transduction using laterally-constrained dielectric elastomers part I: Actuation processes*. J. Mech. Phys. Solids 105: 81-94, 2017.

[18] Hodgins M and Seelecke S. *Systematic experimental study of pure shear type dielectric elastomer membranes with different electrode and film thicknesses*. Smart Mater. Struct. 25: 095001, 2016.

[19] Hossain M, Vu D K and Steinmann P. *A comprehensive characterization of the electro-mechanically coupled properties of VHB 4910 polymer*. Arch. Appl. Mech. 85: 523-537, 2015.

[20] Hossain M, Vu D K and Steinmann P. *Experimental study and numerical modelling of VHB 4910 polymer*. Comput. Mater. Sci., 59:65-74, 2012

[21] Mehnert M, Steinmann P. *On the influence of the compliant electrodes on the mechanical behavior of VHB 4905*. Comput. Mater. Sci., 160:287-294, 2019

[22] Mehnert M, Hossain M, Steinmann P. *Experimental and numerical investigations of the electro-viscoelastic behavior of VHB 4905*. Euro. Jour. Mech. A/Solids, 77(103797), 2019

[23] Liao Z, Yao X H, Zhang L H, Hossain M, Wang J, Zang S G. *Temperature and strain rate dependent large tensile deformation and tensile failure behaviour of transparent polyurethane at intermediate strain rates*. International Journal of Impact Engineering, 129:152-167, 2019

[24] Liao Z, Hossain M, Yao X H, Mehnert M, Steinmann P. *On thermo-viscoelastic experimental characterisations and numerical modelling of VHB polymer*. International Journal of Non-Linear Mechanics, In Review, 2019

[25] Wissler M and Mazza E. *Electromechanical coupling in dielectric elastomer actuators*. Sensors Actuators, A Phys. 138: 384-393, 2007.

[26] Schmidt A, Bergamini A, Kovacs G and Mazza E. *Multiaxial mechanical characterization of interpenetrating polymer network reinforced acrylic elastomer*. Exp. Mech. 51: 1421-1433, 2011.

[27] Goh Y F, Akbari S, Khanh Vo T V and Koh S J A. *Electrically-induced actuation of acrylic-based dielectric elastomers in excess of 500% strain*. Soft Robot. 00, 10.1089/soro.2017.0078, 2018.

[28] Smith T L. *Ultimate tensile properties of elastomers. II. Comparison of failure envelopes for unfilled vulcanizates*. J. Appl. Phys. 35, 1964.

[29] Fan W, Wang Y and Cai S. *Fatigue fracture of a highly stretchable acrylic elastomer*. Polym. Test. 61: 373-377, 2017.

[30] Ahmad D and Patra K. *Fracture behavior of dielectric elastomer under pure shear loading*. IOP Conf. Ser. Mater. Sci. Eng. 229, 2017.

[31] Wang H, Wang K, Fan W and Cai S. *Rupture of swollen styrene butadiene rubber*. Polym. Test. 61: 100-105, 2017.

[32] Setua D K and De S K. *Effect of short fibres on critical cut length in tensile failure of rubber vulcanizates*. J. Mater. Sci. 20: 2653-2660, 1985.

[33] Akhtar S, Bhowmick A K, De P P and De S K. *Tensile rupture of short fibre filled thermoplastic elastomer*. J. Mater. Sci. 5: 4179-4184, 1986.

[34] Hamed G. *Effect of crosslink density on the critical flaw size of a simple elastomer*. Rubber Chem. Technol. 56:244-291, 1983.

[35] Chen C, Wang Z and Suo Z. *Flaw sensitivity of highly stretchable materials*. Extrem. Mech. Lett. 10:50-57, 2017.

[36] Rosset S, Maffli L, Houis S and Shea H R. *An instrument to obtain the correct biaxial hyperelastic parameters of silicones for accurate DEA modelling*. SPIE Smart Structures and Materials, Nondestructive Evaluation and Health Monitoring 9056, 90560M-90560M, 2014

[37] Li B, Zhang J, Liu L, Chen H, Jia S, Li D. *Modeling of dielectric elastomer as electromechanical resonator*. J. Appl. Phys. 116: 124509, 2014.

[38] Moreira D C, Nunes L C S *Comparison of simple and pure shear for an incompressible isotropic hyperelastic material under large deformation*. Poymer Testing. 32: 240-248, 2013.

[39] Ahmad D, Patra K *Experimental and theoretical analysis of laterally pre-stretched pure shear deformation of dielectric elastomer*. Poymer Testing. 75: 291-297, 2019.

[40] Sakulkaew K. Tearing of Rubber. PhD Thesis, Queen Mary Univ. London, 2012.

[41] Marano C, Boggio M, Cazzoni E and Rink M. *Fracture phenomenology and toughness of filled natural rubber compounds via the pure shear test specimen*. Rubber Chem. Technol, 87:501-515, 2014.